OPEN ACCESS

Original research

Extrinsic lipids are absorbed and accumulate in colorectal cancer

Klaus Peter Janssen [1], Marijana Basic,[2] Silvia Bolsega [2], Amira Metwaly [3], Florian Jokisch,[1] Sophia von Gamm [4], Josef Scheiber,[5] Ralph Burkhardt,[6] Gerhard Liebisch,[6] Klaus Neuhaus [3], Sarah Brunner [4], Thomas Clavel [7], Esther Wortmann,[7] Olivia I Coleman,[8] Dirk Haller [8], Andre Bleich,[2] Sabrina Krautbauer,[6] Josef Ecker [4]

► Additional supplemental material is published online only. To view, please visit the journal online (https://doi.org/10.1136/gutjnl-2025-336377).

For numbered affiliations see end of article.

Correspondence to
Professor Josef Ecker; josef.ecker@ukr.de and Professor Klaus Peter Janssen; Klaus-peter.janssen@tum.de

Received 11 July 2025
Accepted 1 March 2026

To cite: Janssen KP, Basic M, Bolsega S, *et al*. *Gut* Epub ahead of print: [*please include* Day Month Year]. doi:10.1136/gutjnl-2025-336377

ABSTRACT

Background Colorectal cancer (CRC) exhibits increased levels of arachidonic acid-derived pro-inflammatory derivatives indicating an uptake of dietary polyunsaturated fatty acids (PUFAs).

Objective We aimed to investigate uptake of extrinsic fatty acids (FAs) in tumours and their relevance for CRC lipid metabolism and progression.

Design Total FAs were quantified using gas chromatography-mass spectrometry in non-diseased mucosa and tumour tissue from patients with CRC of a discovery cohort (n=152), validated in an independent cohort (n=28) and associated with clinical, genomic and microbiome data. The genetic mouse tumour model Apc^{1638N} was used to track the flux of stable isotope-labelled FAs in tumours from the intestinal lumen. The relationship between FA uptake and tumour progression was investigated in 2D and 3D cell models.

Results Extrinsic long chain PUFAs, including arachidonic acid, accumulate in CRC, particularly in right-sided tumours, and in tumours of Apc^{1638N} mice. The CRC-specific FA profiles were independent of sex, molecular subtypes, early-disease or late-disease onset. The absorption of FAs from the intestinal lumen in tumours was confirmed in specific pathogen-free Apc^{1638N} mice. In the absence of the microbiome, in germ-free Apc^{1638N} mice, fewer tumours were developed, and survival was increased. Inhibition of FA import or β-oxidation reduces cancer cell proliferation.

Conclusion Extrinsic FAs accumulate in CRC, verifying a central role of arachidonic acid-derived inflammatory mediators, but also suggesting a relevance of dietary FAs for cancer cell proliferation. It will be intriguing to explore to what extent targeting this flux pathway together with the interrelated microbiome opens new therapeutic avenues for CRC in humans.

WHAT IS ALREADY KNOWN ON THIS TOPIC

⇒ The current understanding of fatty acid (FA) sources for cancer cells is straightforward: FAs originate mainly from intracellular de novo synthesis.

WHAT THIS STUDY ADDS

⇒ Extrinsic, including dietary long chain polyunsaturated fatty acids, FAs are absorbed and accumulate in colorectal cancer (CRC), suggesting a contribution as energetic substrates and membrane components in cancer cells.

HOW THIS STUDY MIGHT AFFECT RESEARCH, PRACTICE OR POLICY

⇒ It will be intriguing to explore to what extent targeting FA uptake and metabolism in cancer cells, for example, by dietary intervention, pharmacological inhibition of FA flux or modulation of the microbiome regulating host lipid metabolism, opens new therapeutic avenues for CRC.

INTRODUCTION

We read with great interest the recent publication by Soundararajan *et al*,[1] reporting on increased levels of arachidonic acid-derived phospholipids, their pro-inflammatory and tumour-promoting derivatives, and an overexpression of genes encoding their biosynthetic enzymes in colorectal cancer (CRC). Since humans cannot generate polyunsaturated fatty acids (PUFAs) from mono-unsaturated fatty acids (MUFAs),[2] those results suggest an uptake of arachidonic acid (FA20:4 n-6) and/or its precursors in cancer cells from the diet.

Fatty acid (FAs) accessibility is key for cancer metabolism. FAs are β-oxidised to generate adenosine triphosphate (ATP) or used for membrane lipids like phosphatidylcholine (PC) or phosphatidylethanolamine (PE), in proliferating cells.[3 4] The current paradigm is that those originate from de novo lipogenesis, which is drastically induced in CRC, but low in non-diseased intestinal tissue. In intestinal tumours, the expression of fatty acid synthase (FASN), a key enzyme in de novo synthesis (DNS) of FAs, is associated with inferior prognosis,[5] and its inhibition is considered for CRC treatment.[6] The downside of high lipogenesis is that it consumes enormous amounts of nicotinamide adeninedinucleotide phosphate (NADPH), an important source of reducing power critical for tumour cell metabolism.[3] Building one molecule palmitate (FA16:0) de novo requires 14 molecules NADPH. Hence, the uptake of extrinsic FAs from

the intestinal lumen, the circulation or the tumour microenvironment[7] might be a simple and opportunistic alternative for DNS. However, the uptake of extrinsic FAs by gastrointestinal cancer cells and its interrelation with endogenous FA biosynthesis are still unclear.

Therefore, we quantified total fatty acids (TFAs) in two independent cohorts of patients with primary CRC, with a particular focus on diet-derived long chain PUFAs. After integration of FA profiles from both cohorts and association with clinical and genetic parameters, an accumulation of extrinsic, most likely diet-derived FAs in tumours was identified. Using in vivo stable isotope-labelling experiments, the flux of extrinsic FAs from the intestinal lumen into tumour tissues was confirmed in a genetic mouse tumour model (Apc^{1638N}). To explore the role of the microbiome involved in CRC development and FA metabolism, germ-free (GF) Apc^{1638N} were bred, as well as the faecal and tumour tissue microbiome composition was investigated in patients.

MATERIAL AND METHODS

All materials used and methods applied are described in detail in the online supplemental methods.

Human tissue samples

The discovery cohort consisted of n=152 patients, and the validation cohort of n=28 patients with primary CRC, who underwent surgery and gave informed consent for analysis of their tissue and data at the Department of Surgery (TUM, Munich) between 1987 and 2024. Patients with neoadjuvant treatment were excluded and only cases with curative tumour resection (R0) were included, except for UICC/AJCC (Union for International Cancer Control/American Joint Committee on Cancer) stage IV patients, who presented synchronous distant metastasis at first diagnosis. Tissue samples were macro-dissected to separate carcinoma from adjacent non-tumour tissue and immediately shock-frozen in liquid nitrogen. Tumour cellularity (>70%) was assessed by histology-guided sample selection, based on histological evaluation of H&E stained consecutive tissue cryo-sections.[5] Briefly, the first and last of consecutive cryo-sections were mounted on glass slides and processed for histology, the intermediate sections were sampled in tubes and used for FA analyses. Clinical characteristics are summarised in table 1; representative histology is shown in online supplemental figure 1.

Mouse models and housing

GF and specific pathogen-free (SPF) Apc^{1638N} mice (male and female, ~1:1; mean age: 8 months) were exposed to a 12 hours light-dark cycle, housed at 22°C and fed a chow diet. Breeding of GF mice was performed in plastic film isolators, SPF mice were housed in individually ventilated cages.

Stable isotope labelling of lipid uptake and flux in mice

10–16 weeks old SPF Apc^{1638N} mice (male) were starved for 2 hours before oral gavage of 100 µL of olive oil containing 10 µmol FA16:0[D5] (Hexadecanoic-15,15,16,16,16-d_5 Acid), 3.33 µmol TG(16:0[D31])$_3$ (Glyceryl-Tri(hexadecanoate-d_{31})) (CDN isotopes) and 476 µmol FA2:0[13C]$_2$. After 1–2-6 hour mice were sacrificed.

Table 1 Clinical parameters for human CRC cohorts CI and CII

Parameter	Variable	Discovery cohort/CI, n=152	Discovery cohort/CI, proportion (%)	Validation cohort/CII, n=28	Validation cohort/CII, Proportion (%)
Sex	Male	90	59	15	54
	Female	62	41	13	46
Age	Mean/median and range (years)	Mean 64.2/Median 66; 30–86		Mean 66.7/Median 67; 48–88	
Histology (WHO)	Adenocarcinoma	133	88	28	100
	Mucinous carcinoma	16	10.5	0	0
	Signet ring carcinoma	3	1.5	0	0
pTNM-stage (UICC/AJCC)	I	7	5	7	25
	II	38	25	8	29
	III	83	55	6	21
	IV	24	16	7	25
Anatomical localisation	Left-sided colon	75	49	15	54
	Right-sided colon	70	46	9	32
	Rectum	7	5	4	14
Alive status	Alive	60	39	13	46
	Tumour-related death	45	30	1	4
	Non-tumour-related death	38	25	0	0
	Lost to follow-up	9	6	14	50
Recurrence	No recurrence	76	50	9	32
	Disease recurrence	51	34	5	18
	Lost to follow-up	25	16	14	50
Non-diseased control tissue	Matched controls (colorectal mucosa)	100	66	28	100

pTNM: staging system; UICC/AJCC; Union for International Cancer Control/American Joint Committee on Cancer.
CRC, colorectal cancer.

TFA analysis

TFA analysis was performed by gas chromatography coupled to mass spectrometry (GC-MS) of FA methyl esters.[8 9] FAs were quantified by single ion monitoring (SIM), to detect specific fragments of saturated (74 m/z), mono-unsaturated (55 m/z), di-unsaturated (67 m/z) and polyunsaturated FA (79 m/z). Isotopically-labelled FAs were quantified by SIM of molecular ions using the calibrations of unlabelled species (internal standard: C21:0iso).

Mass isotopomer distribution analysis

To determine de novo FA synthesis, enrichment of $^{13}C_2$ in FA16:0 was analysed by mass isotopomer distribution analysis (MIDA) using SIM of molecular ions (M: 270 m/z; M2–M16: 272–286 m/z).[9–11] Fractional synthesis rates (FSRs) representing the fraction of newly synthesised FA16:0 were calculated using the excess mass ratio of the isotopologues M6/M4 relative to an unlabeled control.

Statistical analyses of lipidomic data

Lipid data were analysed according to the principles described previously.[9] For the generation of volcano plots, all data were $\log_2$ transformed. Lipid species were excluded if undetectable in more than 50% of samples. An unpaired t-test assuming unequal variances was used to test for significantly different abundances in the conditions. The Benjamini-Hochberg method was used to calculate the false discovery rate (FDR) and to account for multiple testing ($p_{adj} < 0.05$). Fold changes were calculated as the difference between the mean of the $\log_2$-transformed values of the respective groups. To compare mean lipid concentrations between groups, an unpaired t-test assuming unequal variances was applied.

Overall survival rates after surgery were analysed using a multivariate Cox regression with adjustments for age, sex, UICC tumour stage and anatomical localisation of CRC (right-sided or left-sided).

Cell culture (2D and 3D) and assays

Proliferation of human CRC 2D cell lines, HCT116 (RRID: CVCL_0291) and DLD1 (RRID: CVCL_0248) (ATCC, Rockville, Maryland, USA) was determined by analysis of mitochondrial activity[12] after incubation with SMS121 or etomoxir (Biozol) for 24 hours, compared with solvent control (DMSO). 3D organoids were generated from n=5 patients with primary CRC.[13] Viability was tested using resazurin (Sigma-Aldrich)[12] after incubation with SMS121 or etomoxir for 96 hours.

Microbiome analyses in stool and tissue samples

Tumour tissue and matched adjacent normal tissue samples were collected from 26 patients with CRC (CII) during surgical resection, and stool samples were collected from 18 patients with CRC (CII) prior to treatment. After extraction of bacterial DNA,[14] the V3–V4 region of the 16S rRNA gene was sequenced (tissue), or shallow shotgun metagenomic sequencing was performed (stool).

RESULTS

Study design and cohort characteristics

The discovery cohort, referred to as cohort I (CI), consisted of 152 patients with primary CRC with a median follow-up of 80 months with tumour and matched normal tissue available for 87 patients. An independent validation cohort, referred to as CII, comprised 28 additional patients with CRC with matched tumour and normal samples. In addition, blood plasma (20 patients) and stool samples (18 patients) were available in CII. Clinical data are indicated in table 1 and representative histology is shown in online supplemental figure 1.

Long-chain and PUFAs accumulate in CRC

To improve our understanding of CRC FA metabolism, we quantified TFAs containing 8–24 carbons including PUFAs (online supplemental table 1) using GC-MS in CI. Comparing tumour tissue with normal mucosa, we identified systematic discrepancies. FAs containing >18 carbons and >3 double bonds (DBs) including FA20:4 n-6 were enriched in tumours, while shorter saturated and mono-unsaturated species like FA16:0 (palmitic acid) and FA18:1 n-9 (oleic acid) were depleted compared with normal tissue (figure 1A–C, unmatched comparison of n=152 patients; online supplemental figure 2, matched comparison of n=87 patients). To verify these results, TFAs were quantified in an independent cohort (CII) using the identical method as for CI. Here, the comparison of matched normal and tumour samples revealed almost the identical changes between tumour tissue and normal mucosa as observed in CI (figure 1D–F). The ratios between FA20:4 n-6 and FA22:6 n-3 were similar in normal mucosa and CRC tumours of both cohorts (figure 1C and F). In total, in CI and CII, eight TFA species were consistently higher abundant in tumours including FA20:4 n-6 (figure 1G, Q2), and seven were consistently higher abundant in normal tissue (figure 1G, Q4). An exploratory survival analysis (with adjustments for age, sex, UICC tumour stage and anatomical CRC localisation; but no other clinical confounders) based on the postoperative follow-up data obtained in CI and CII (n=94 patients) revealed that low FA20:5 n-3 levels were associated with lower overall year survival postsurgery (p=0.007; online supplemental figure 3). FA22:6 n-3 levels correlated between tumour and blood plasma (n=20 patients from CII) with R=0.77 and p<0.001 (online supplemental table 2; online supplemental figure 4).

In accordance with human CRC, very similar FA patterns, with elevated fractions of C20–C24 FA containing >3 DB including FA20:4 n-6 were detected in tumours of a genetic mouse model for human CRC, the Apc^{1638N} line[5 15] (figure 1H–J), indicating conserved tumour FA signatures across different species.

Comparison of FA profiles in right-sided and left-sided CRC

The anatomical localisation of CRC is well known to have prognostic and predictive relevance. It affects their molecular profiles (eg, frequency of microsatellite instability (MSI) and B-Raf proto-oncogene (BRAF) mutations) and the expression of lipid-related enzymes.[16 17] Patients with right-sided colon cancer have an inferior prognosis compared with left-sided colon cancer,[18] especially in advanced disease stages. In CI and CII (combined datasets), the abundances of FA22:0, FA23:0, FA24:0, FA24:1 n-9, FA20:3 n-6, FA20:4 n-6 and FA22:4 n-6 were significantly elevated in right-sided compared with left-sided tumours (including rectal cancer) (figure 2A–C). Here, the ratios between FA20:4 n-6 and FA22:6 n-3 were 20% higher in right-sided CRC, which is reasonable considering that right-sided CRC tends to be more aggressive, most likely containing higher amounts of pro-inflammatory metabolites. Also, in right-sided, but not left-sided tumours, the levels of C20–C24 and fourfold unsaturated FAs increased from UICC/AJCC stage III (lymph node metastasis) to stage IV (distant metastasis) (online supplemental figure 5).

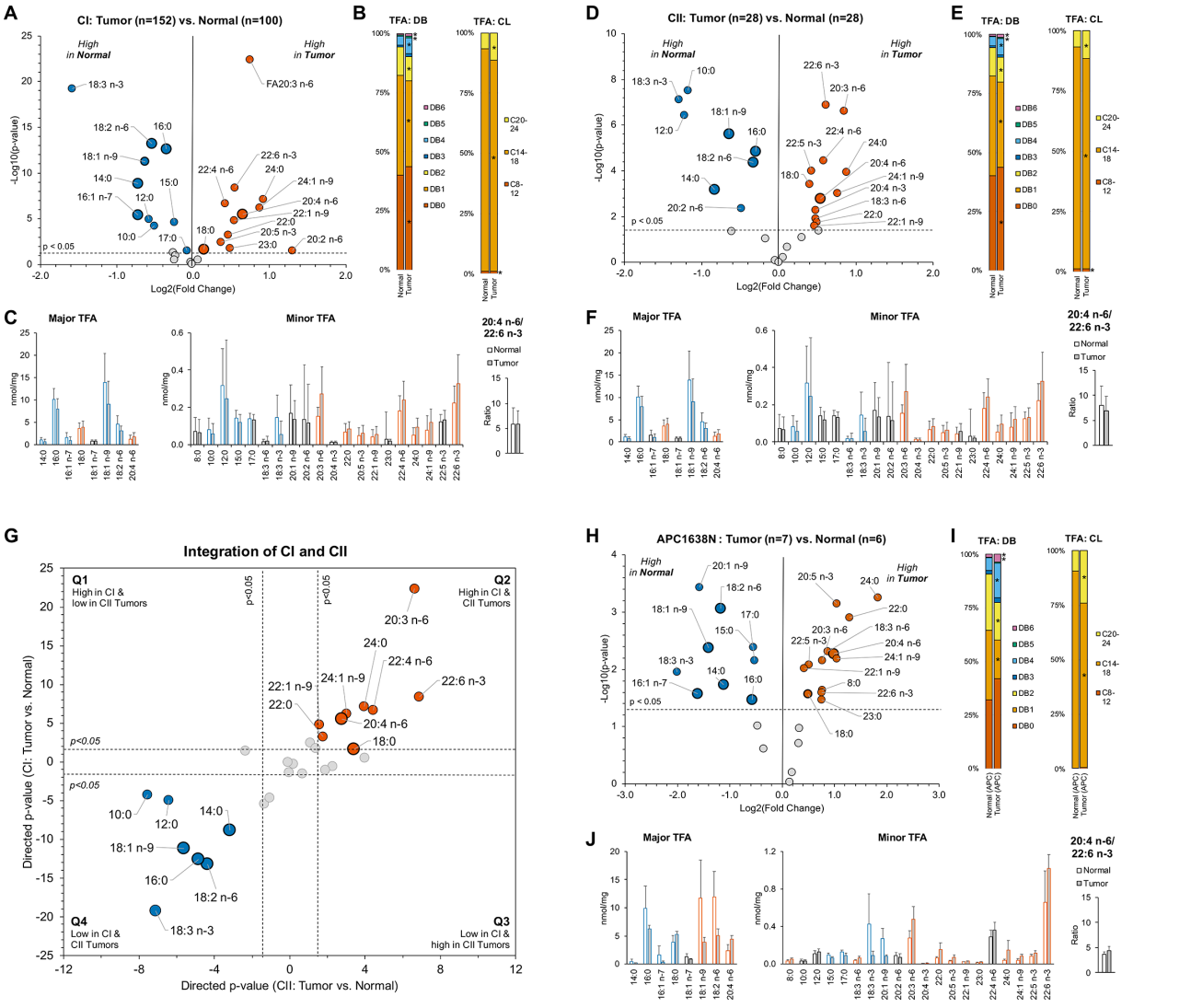

Figure 1 Extrinsic FAs accumulate in human CRC and tumours of APC^{1638N} mice. (A–F) Differential analysis of TFA species in tumour (CI: n=152; CII: 28) versus non-diseased samples (CI: n=100; CII: n=28) of the human CRC cohorts CI and CII. (G) Integration of significant different TFAs identified in the comparisons tumour versus non-diseased samples in CI and CII. Directed p values are defined as '–log10 (p) times the direction of the effect'. (H–J) Differential analysis of tumour (n=7) versus non-diseased tumour-adjacent samples (n=6) from APC^{1368N} mice. Volcano plots display FAs, whose concentrations are significantly changed between the groups (A, D, H). Enlarged dots indicate major FAs. p<0.05 after correcting for multiple testing by controlling the false discovery rate at 5%. Stacked column charts indicate the distribution of the major and minor TFAs according to their number of carbons and double bonds (DBs) (B, E, I). Bar plots show the levels of the major and minor FA species, and the ratios of FA20:4 n-6 and FA22:6 n-3 as means+SD (C, F, J). Coloured bars (orange: high in tumours, blue: low in tumours) or * indicate a significant difference at p<0.05, determined using an unpaired Student's t-test. CL, chain length; CRC, colorectal cancer; FA, fatty acid; TFA, total fatty acid.

To investigate whether genetic tumour subtypes influence the accumulation of long chain and PUFAs in CRC, the lipidomic data were stratified by oncogenic KRAS exon 2 mutations, BRAF exon 15 mutations and the DNA MSI status. We could not find associations with KRAS mutation (online supplemental figure 6) or MSI status (online supplemental figure 7), but increased levels of FA22:0, FA 23:0 and FA20:4 n-6 in tumours with BRAF^{V600E} mutations compared with BRAF wildtypes (online supplemental figure 8A-C). Since BRAF-mutated tumours are typically found in the right-sided colon[16] (9 of the 10 BRAF-mutated tumours were right-sided), we analysed after stratification for BRAF mutations in right-sided normal tissue and tumours (online supplemental figure 8D-F). In this subgroup analysis, no differences between wildtype and tumours with BRAF^{V600E} mutations could be detected, indicating that rather the anatomical location (figure 2A) than the BRAF oncogene might determine the tumour's FA profiles.

Long-chain PUFA enrichment in tumours independent of sex and similar in early-onset and late-onset CRC

Sex can influence both lipid metabolism[19–21] and CRC pathophysiology. Female patients have a survival advantage[22] and are more likely to develop right-sided CRC.[18] In accordance, in both cohorts (CI and CII), the proportions of right-sided tumours (including rectal) were 63% in women and 39% in men. Consequently, we asked whether the differences observed in TFAs between CRC and normal tissues depend on sex by analysing the datasets from male and female patients separately. In men, 20 (of 28) TFAs were significantly differently abundant between

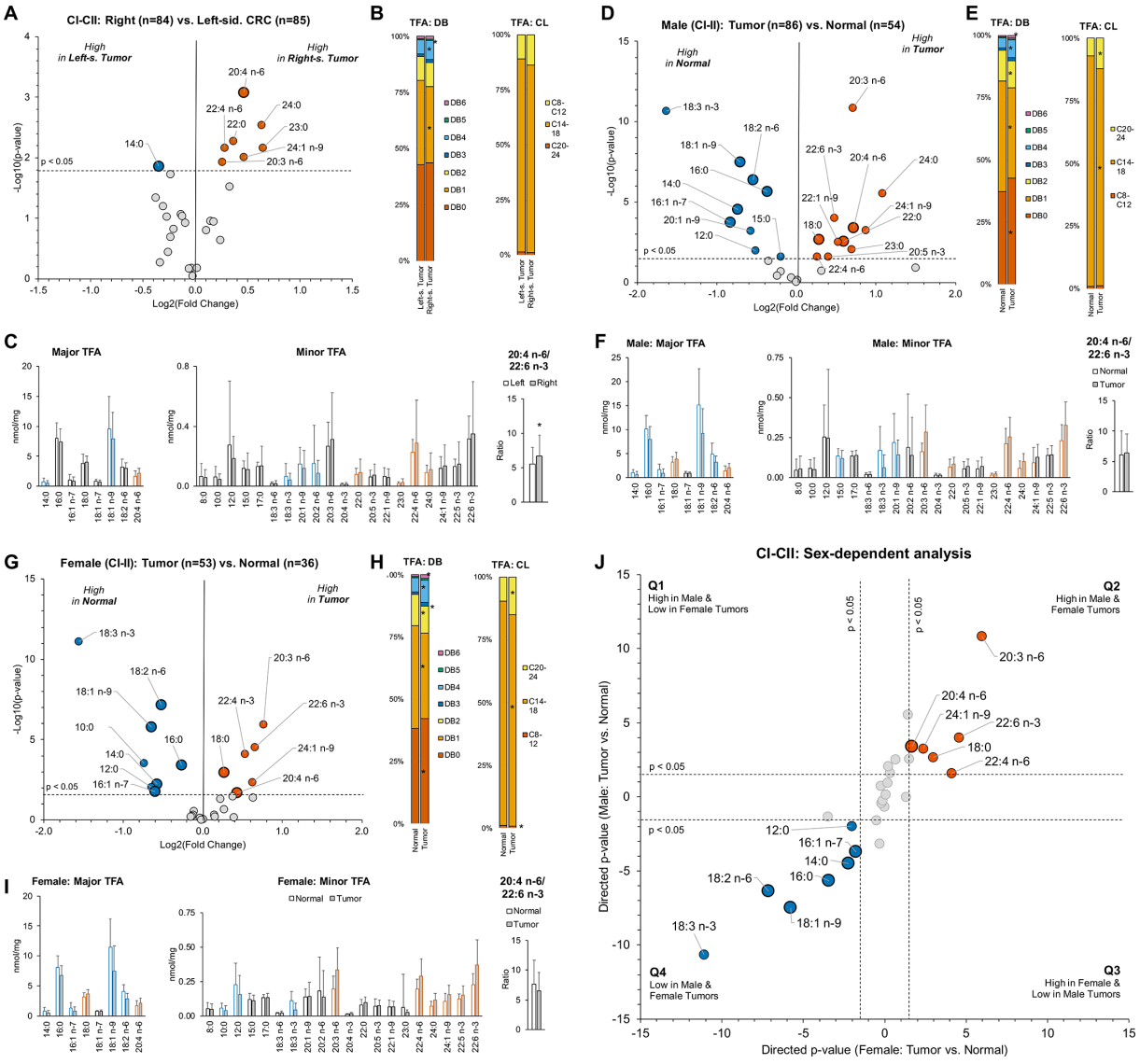

Figure 2 Comparison of FA profiles in right-sided and left-sided CRC and sex-dependent analyses. (A–C) Differential analysis of TFA species in right-sided (n=84) versus left-sided tumours (n=85) of the combined datasets of CI and CII. (D–E) Differential analysis of TFA species in tumour (n=86) versus non-diseased samples (n=54) of male and (G–I) in tumour (n=53) versus non-diseased samples (n=36) of female patients of the combined datasets of CI and CII. (J) Integration of significant different TFAs identified in the comparisons of tumour versus non-diseased samples of male and female patients in CI and CII. Directed p-values are defined as '–log10 (p) times the direction of the effect'. Volcano plots display FAs, whose concentrations are significantly changed between the groups (A, D, G). Enlarged dots indicate major FAs. p<0.05 after correcting for multiple testing by controlling the false discovery rate at 5%. Stacked column charts indicate the distribution of the major and minor TFAs according to their number of carbons and double bonds (DBs) (B, E, H). Bar plots show the levels of the major and minor FA species, and the ratios of FA20:4 n-6 and FA22:6 n-3 as means+SD (C, F, I). Coloured bars (orange: high in tumours, blue: low in tumours) or * indicate a significant difference at p<0.05, determined using an unpaired Student's t-test. CL, chain length; CRC, colorectal cancer; FA, fatty acid; TFA, total fatty acid.

tumour and normal samples (figure 2D–F), while in women 'only' 14 TFAs (of 28) differed (figure 2G–I), which might be most likely due to the smaller sample size (resulting in a lower statistical power) available for female patients. Most importantly, in tumours of both groups, TFAs containing C20–C24 and PUFAs (≥4 DB) including FA20:4 n-6 and FA22:6 n-3 were accumulated in tumours, while C12–C14 saturated and mono-fold, di-fold and tri-fold unsaturated C18 FAs were depleted (figure 2J, Q2 and Q4). The finding that no TFA species showed significant different changes between men and women (figure 2J, Q1 and Q3) indicates no major sex-based differences.

To test if the tumour-specific changes in TFA differ between late-onset CRC (LOCRC) and early-onset CRC (EOCRC), which shows an increasing incidence in the last decade,[23] we split the combined datasets of CI and CII into the subgroups of patients, when CRC was diagnosed under or above the age of 50 years. Although in LOCRC, the number of significant different TFA species was higher (also most likely due to the higher sample size of n=166 tumours and n=112 normal; online supplemental figure 9A-C) than in EOCRC (of n=23 tumours, n=16 normal; online supplemental figure 9D-F), the fundamental alterations with elevations of FA20:3 n-6, FA20:4 n-6, FA22:4 n-6, FA24:0 and FA24:1 n-9 and reduction of FAs containing 14–18 carbons were similar in both subgroups (online supplemental figure 9G). No TFA species show different changes between the subgroups EOCRC and LOCRC.

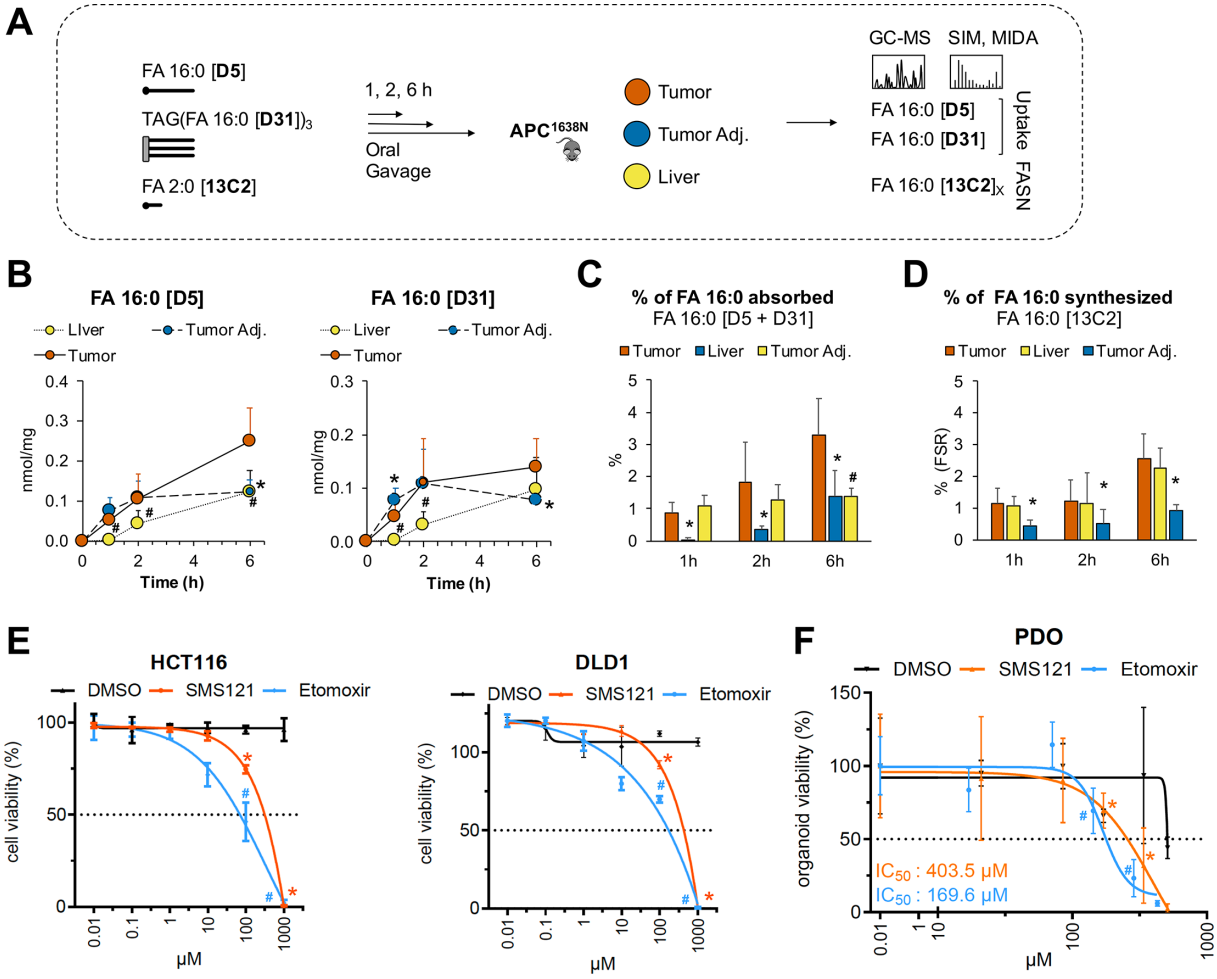

Figure 3 Extrinsic FAs are absorbed in tumours of Apc^{1638N} mice and required for CRC cell proliferation (A) Experimental strategy to determine exogenous FA uptake and endogenous FA synthesis in tumours, tumour-adjacent and liver samples of APC^{1368N} mice. At 1–6 hours after oral gavage of mice with FA16:0[D5], TG(16:0[D31])$_3$ and FA2:0[13 C2] mice were sacrificed. (B) FA16:0[D5] and FA16:0[D31] levels and (C) percentage contribution of FA16:0[D5] and FA16:0[D31] relative to total FA16:0. (D) Fractional [13 C2] enrichment in FA16:0 (fractional synthesis rate, FSR). Means+SD of: n=8 (1 hour), n=5 (2 hours), n=6 (6 hours) for liver; n=12 (1 hour), n=16 (2 hours), n=12 (6 hours) for tumour tissue and n=10 (1 hour), n=10 (2 hours), n=8 (6 hours) for tumour-adjacent tissue. */$^{\#}$p<0.05, unpaired Student's t-test, tumour-adjacent (*) or liver ($^{\#}$) compared with tumours. (E) Viability of HCT116 and DLD1 cells treated with SMS121 (CD36 inhibitor) or etomoxir (Cpt1a inhibitor) for 24 hours at the indicated concentrations compared with DMSO-treated controls (n=3 per group and concentration). (F) Viability of patient-derived organoids (PDO) derived from five patients with CRC treated with SMS121 or etomoxir for 96 hours at the indicated concentrations compared with DMSO-treated controls (n=3 per group and concentration). IC$_{50}$-values were calculated in Graph Pad Prizm using a variable slope with four parameters. */$^{\#}$p<0.05, unpaired Student's t-test, SMS121 (*) or etoxomir ($^{\#}$) compared with the DMSO control. CRC, colorectal cancer; FA, fatty acid; FASN, fatty acid synthase; GC-MS, gas chromatography coupled tomass spectrometry; MIDA, mass isotopomer distribution analysis; SIM, single ion monitoring.

Extrinsic FAs are absorbed in tumours of Apc^{1638N} mice and required for CRC cell proliferation

The long chain C20–C24 PUFAs containing 4–6 DB found enriched in human CRC and tumours of the Apc^{1638N} mouse model must derive from extrinsic sources, most likely diet. MUFAs, which are an end product of FA DNS (online supplemental figure 10), cannot be di-saturated to obtain PUFAs in mammalians.[2] To functionally confirm an (1) uptake of lipids from the intestinal lumen in tumours, Apc^{1638N} mice were gavaged with deuterated palmitate (FA16:0[D5]), tripalmitin (TG(16:0[D31])$_3$) and (2) [$^{13}C_2$]-labelled acetate (FA2:0[$^{13}C_2$]) (figure 3A) to determine enrichment of [$^{13}C_2$]-labelled C2 units in FA16:0 as measure for FA DNS. We found (1) a time-dependent uptake of FA16:0[D5,D31] in tumours. At 6 hour, 3.3% of total FA16:0 originated from absorption (FA16:0[D5] and FA16:0[D31]) in tumours and FA16:0[D5] levels were twofold higher than in tumour-adjacent normal intestinal tissue and liver (figure 3B,C). (2) DNS was threefold higher in tumours than in non-diseased adjacent tissue, and comparable to the liver, which has the largest capacity for lipid synthesis in the body (figure 3D). Here, 2.6% of total palmitate was newly synthesised in 6 hours, shown by the FSR calculated using MIDA, indicating that DNS and uptake of palmitate contribute approximately equally to the tumour's FA pool. When FA2:0[$^{13}C_2$] was removed from the lipid mix gavaged to the mice, the uptake of FA16:0[D5,31] into tumours increased twofold (online supplemental figure 11), suggesting that FA absorption is balanced with DNS in cancer cells.

To test the relevance of extrinsic FA for CRC cell proliferation and survival, we incubated two established CRC cell lines and primary patient-derived organoids (PDO) with SMS121, a pharmacological inhibitor of FA translocase CD36 involved in

cellular FA import,[24 25] or etomoxir, inhibiting carnitine palmitoyltransferase 1A (CPT1a) and FA oxidation.[26] In HCT116 and DLD1 cell lines, viability was reduced with increasing concentrations of both inhibitors compared with mock-treated cells (figure 3E). At 100 µM, SMS121 reduced viability in both cell lines by ≈50% (reported IC_{50}: 156–164 µM in cells[24] and etomoxir by ≈25% (reported IC_{50}: 0.1–10 µM in isolated mitochondria and cells.[26] Similarly, in PDOs, viability was inhibited with increasing concentrations of SMS121 (calculated IC_{50}: 403.5 µM) and etomoxir (calculated IC_{50}: 169.6 µM) compared with mock-treated cells (figure 3F).

Together, these results provide strong evidence that extrinsic FAs are taken up in CRC tumours and required for cancer cell proliferation and thus are critical for CRC metabolism and tumour progression.

The presence of the microbiome drives tumour development in Apc^{1638N} mice, but its faecal and tissue-associated composition is heterogenous in patients with CRC

Since the gut microbiome is involved in intestinal lipid absorption[27–30] and host DNA,[9] we asked whether tumour formation depends on its presence. In fact, we could detect lower numbers of intestinal tumours (figure 4A), reduced splenomegaly (figure 4B) and mortality in GF compared with SPF Apc^{1668N} mice harbouring a diverse gut microbiome (figure 4C). Splenomegaly, the enlargement of the spleen's size and weight, is a result of extramedullary haematopoiesis compensating for the blood loss due to bleeding of intestinal tumours. It is well known to be related to the intestinal tumour load in patients and Apc-mutant mouse models.[15]

Also, in humans, accumulating evidence indicates the microbiota as an important player in the development and progression of CRC. Hence, we characterised the faecal and tumour tissue-associated microbiome in patients with CRC (CII). Shallow metagenome sequencing of stool samples from 18 patients with CRC revealed wide inter-individual variation in alpha diversity and substantial heterogeneity in taxonomic composition at both family and species levels (online supplemental figure 12A). PCoA ordination demonstrated dispersed clustering with the first two principal coordinates explaining only 25.3% of variance, confirming high inter-patient variability (online supplemental figure 12B). At the family level, *Bacteroidaceae*, *Oscillospiraceae*, *Lachnospiraceae* and *Ruminococcaceae* dominated most samples, though *Enterobacteriaceae* showed sporadic enrichment in individual patients (online supplemental figure 12C). Species-level analysis identified high compositional heterogeneity, with patient-specific dominance patterns (online supplemental figure 12D). Core microbiome analysis (80% prevalence threshold) identified *F. prausnitzii*, *P. vulgatus*, *B. thetaiotaomicron* and *B. uniformis* as most prevalent species (>60%), though with variable abundances across patients (online supplemental figure 12E).

In tissue samples, comparison of bacterial community compositions between tumour (n=26) and adjacent normal tissue (n=22) samples after 16S rRNA amplicon sequencing demonstrated a similar alpha diversity including richness and Shannon effective number of species (figure 4D and E). Non-metric multidimensional scaling ordination of Bray-Curtis dissimilarities demonstrated substantial overlap between both groups (figure 4F). The type of tissue analysed (normal or tumour tissue) explained only 2.6% of variance in community composition (R^2=0.026, p=0.25), suggesting a high inter-individual variability rather than consistent group-level separation. At the phylum level, the tissue-associated microbiome was dominated by *Bacillota* (60%–65%) and *Bacteroidota* (20%–25%), with a notable heterogeneity in *Pseudomonadota* abundance in tumour samples (range: 2%–40%) compared with normal tissue (range: 5%–15%) (figure 4G). At the family level, *Enterobacteriaceae* were sporadically enriched in a subset of tumour samples (up to 60% compared with <5% in normal tissue), suggesting opportunistic colonisation events rather than universal tumour-specific enrichment (figure 4H). Among the top 15 differentially abundant genera (figure 4I) *Escherichia-Shigella* exhibited the largest effect size among tumour-enriched genera with approximately 10-fold higher mean abundance in tumour samples (though not reaching statistical significance after FDR correction). Other tumour-enriched genera included *Bacteroides*, *Enterococcus*, *Streptococcus* and *Fusobacterium*, while normal tissue showed enrichment of butyrate-producing genera including *Faecalibacterium*, *Dialister* and *Eubacterium eligens group*.

To identify potential microbes affecting CRC FA metabolism, we finally correlated bacterial genus abundances with the validated TFA species differing between normal mucosa and CRC tissue (figure 4J). Among seven genera of interest (*Holdemanella*, *Prevotella*, *Prevotella_7*, *Intestinibacter*, *Bilophila*, *Family XIII AD3011 group*, *Subdoligranulum*), we found significant associations (FDR<0.10) including negative correlations of *Prevotella* with FA10:0 (R=−0.44, p=0.018), FA12:0 (R=−0.50, p=0.005), FA18:2 n-6 (R=−0.45, p=0.015); and *Intestinibacter* with FA22:6 n-3 (R=−0.46, p=0.013).

We conclude that microbiome impacts CRC development and progression in the Apc^{1638N} mouse model. In patients, microbiome diversity and composition are comparable between healthy intestinal tissue and CRC tumours, but patient-specific, leading to substantial tumour-associated microbiome heterogeneity.

DISCUSSION

Cancer metabolism is geared toward biomass production, fueled by glucose as carbon source and by FAs that can be β-oxidised to generate ATP or used for membrane lipids in proliferating cells.[3 4] The current understanding of FA sources for cancer cells is straightforward: FAs originate mainly from intracellular DNS. Here, we show that extrinsic, that is, dietary FAs, are absorbed and accumulate in CRC. Our results not only suggest a contribution of extrinsic FAs as energetic substrates and membrane components in cancer cells,[4] but also verify the central role of arachidonic acid in tumours as precursor for pro-inflammatory mediators reported by Soundararajan and colleagues.[1]

So far, most lipidomic studies focused on mass spectrometry-based profiling of the blood's lipidome aiming to diagnose CRC.[31] In tumour tissues, the majority of reported CRC-specific alterations of lipids are in agreement with our data, although there is a certain heterogeneity and variation between the individual studies published. Consistent datasets include: elevated percental proportions of triglycerides containing polyunsaturated acyl chains (TG56:4, TG56:5, TG56:6) in CRC tumour tissues, which could even be related to patient survival (three cohorts; ∑=154 patients; own investigations reported previously)[5]; increased concentrations of FA20:4 and FA22:6-containing lysophospholipids (eg, lyso-phosphatidylinositol (LPI) 20:4, LPI22:6, lyso-phosphatidylserine 22:6, lyso-phosphatidylglycerol 22:6) in tumour tissues (one cohort; 11 patients)[32]; higher percental proportions of saturated and mono-unsaturated C20, C22 and C24-FAs in CRC tumours (one cohort; 19 patients)[33]; analysis of PC 36:4 (potentially containing FA20:4) signal abundances allowing a discrimination of CRC from normal tissue (20

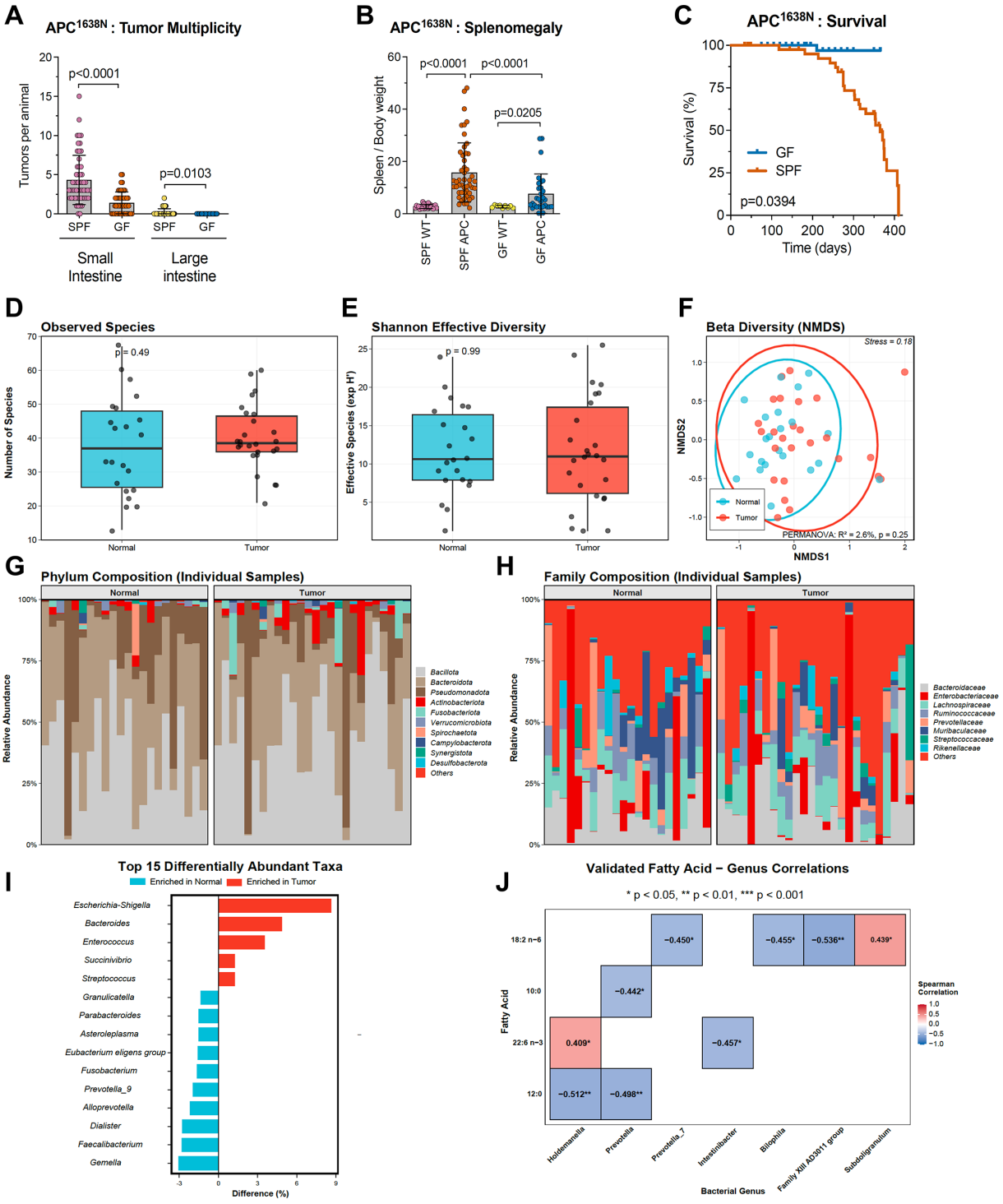

Figure 4 The presence of the microbiome drives tumour development in Apc^{1638N} mice, and normal tissue-associated and tumour-associated microbiome composition in patients with CRC. (A) Numbers of tumours in small and large intestine and (B) ratios of spleen/body weight of SPF and germ-free (GF) Apc^{1638N} mice. Splenomegaly is an established marker of tumour-induced morbidity. Means+SD of n=75 SPF and n=60 GF Apc^{1638N} mice, p values are indicated, determined using an unpaired Student's t-test. (C) Overall survival of GF and SPF Apc^{1638N} mice. (D) Observed species richness in normal (n=22) and tumour (n=26) tissue of CRC patients. (E) Shannon effective diversity (exp H') in normal and tumour tissue of CRC patients. (F) Non-metric multidimensional scaling (NMDS) ordination of bacterial community composition based on Bray-Curtis dissimilarity. Blue=normal, red=tumour. Ellipses represent 95% CIs. (G) Phylum-level taxonomic composition of individual patient samples. (H) Family-level taxonomic composition of individual patient samples. (I) Top 15 differentially abundant genera ranked by absolute difference in mean relative abundance. (J) Spearman correlations between seven bacterial genera and TFA measurements across all patient samples (n=48). Only significant correlations are shown (FDR <0.10; Red: positive correlation, blue: negative correlation). Colour intensity reflects correlation strength. Prevotella and Prevotella_7 are different bacterial entities (different species/OTUs within the Prevotella genus). APC, adenomatous polyposis coli; CRC, colorectal cancer; FDR, false discovery rate; GF, germ-free; SPF, specific-pathogen free.

patients).[34] Divergent findings include: Reduced FA20:5 n-3 and FA22:6 n-3, but elevated FA20:4 n-6 levels in CRC tumour tissues (one cohort; 35 patients)[35]; reduced signal intensities of C20:4-containing lipids and PC38:4 (potentially containing 20:4) in the cancerous areas of intestinal samples from patients with CRC (one cohort; n=6).[36]

Among all PUFAs changed in CRC, only FA18:2 n-6 and FA18:3 n-3, which are the initial precursors of longer and more unsaturated n-3 and n-6 PUFAs (online supplemental figure 10), were found decreased in tumour tissues of CI and CII. This might be due to increased expressions of FA elongase and desaturases (fatty acid elongase 5, fatty acid desaturase (FADS)1 and FADS2) in CRC tumours,[5] generating FA20:4 n-6 and FA22:6 n-3 (both increased in tumour tissue). Deletion of FADS1 in cell lines and mice suppresses tumour cell proliferation, migration and invasion, while promoting apoptosis.[37] In CII, FA22:6 n-3 levels correlated in tumours and plasma, which may reflect to a certain extent its dietary intake. FA22:6 n-3 can be regarded as a reliable and accurate biomarker for n-3 intake in humans,[38] most likely because it is a steady end-product of mammalian n-3 PUFA metabolism (online supplemental figure 10). Unfortunately, dietary histories including PUFA consumption through food frequency questionnaires, as common in dietary intervention studies, are not available for the patients with CRC, because they were included in our study cohorts on surgical tumour resection.

Dietary lipids found enriched in CRC may reach tumour tissues (I) after absorption in the small intestine and transport via blood and lymph vessels or (II) by direct uptake from the colon lumen containing ≈6-8 g of lipids (adults, western diet) that have not been absorbed in the small intestine.[39] The finding that the abundances of the PUFAs FA20:3 n-6, FA20:4 n-6 and FA22:4 n-6 were significantly elevated in right-sided compared with left-sided tumours implies the latter, since the right colon is in closer proximity to the small intestine and thus may have an increased access to lipids. In addition, the different FA profiles between right-sided and left-sided CRC may reflect individual lipid metabolic capacities and requirements. Right-sided tumours deviate from different embryonic tissue origins than left-sided and tend to be of more aggressive phenotype with enhanced proliferative and metastatic potential,[16] with a potentially higher demand for lipids. Also, the transcriptomic landscape of lipid metabolism-related genes differs between right-sided and left-sided CRC,[16 40] and targeting lipid metabolism by chemo-preventive strategies was found to yield different outcomes in left-sided and right-sided CRC.[40]

As the gut microbiome influences intestinal lipid absorption[27–30] and host lipid metabolism,[9] GF Apc^{1638N} mice were bred developing less tumours leading to an increased survival. In agreement, a reduced development of intestinal tumours was observed in APC^{Min} mouse models, when housed under GF conditions or treated long-term with broad-spectrum antibiotics.[41–43] Also, we have previously demonstrated a critical role of the gut microbiome in colonic lipid metabolism of mice transgenic for ATF6 (nATF6^{IEC}), another mouse model for CRC.[44] How the gut microbiota promotes CRC is not fully understood. In our view, a combination of multiple factors might explain the lower numbers of tumours observed in GF APC^{1638N} mice, including: (1) a lower capacity for degradation of complex carbohydrates to acetate,[9] needed for synthesis of membrane lipids of cancer cells, as well as to butyrate fueling hyperproliferation,[43] (2) a lower availability of extrinsic FAs that can be β-oxidised for ATP production and (3) the absence of microbe-associated molecular patterns sensed by toll-like receptors triggering inflammation and colonic tumourigenesis.[45 46]

In patients, we found a substantial inter-individual variation in both faecal and tumour tissue-associated microbiome composition, consistent with growing evidence that CRC microbiomes are patient-specific rather than universally altered.[47] Some tumours showed a strong enrichment of *Escherichia-Shigella*, typically abundant in colon and considered as CRC pathogens promoting tumour formation.[48 49] While a high heterogeneity of the CRC-associated tissue microbiome between patients is well known,[50] alpha diversity analyses revealed inconsistent results between different studies, with either a similar microbial alpha diversity in adjacent non-diseased and CRC tissue (as observed here) or a lower alpha diversity of the CRC tissue-associated microbiome.[50 51] These discrepancies might be due to methodical differences (ie, in sampling and sequencing) or due to the patients (eg, differing in tumour stages and anatomical locations of CRC) included in the study cohorts. A critical factor explaining the reported heterogeneity of the CRC-associated microbiome might be patient-specific immunoinflammatory responses to CRC.[52] Correlation analyses in normal and tissue samples identified negative associations of TFAs (FA10:0, FA12:0, FA18:2 n-6 or FA22:6 n-3) changed in CRC with *Prevotella* and *Intestinibacter*. It is unknown whether these FAs alter bacterial growth or are metabolised by the bacteria before entering host metabolic pathways,[53] but this is certainly of interest, since a bacterial conversion in bioactive molecules could influence inflammation in CRC. Together, our human microbiome results are exploratory, hypothesis-generating and may require further functional validation. However, whether *Prevotella* and *Intestinibacter* critically influence CRC FA uptake and can be used for therapy might be interesting for future investigations, although a relevance was described previously. Faecal *Prevotella copri* was found over-represented in patients with CRC,[54] and *Prevotella intermedia was* enriched in CRC tissue, enhancing migration and invasion of CRC cells.[55] *Intestinibacter* was reported to be more abundant in faecal samples of patients with colorectal adenomas compared with healthy controls[56] and positively associated with CRC risk.[57]

In summary, our findings extend the current understanding of CRC FA metabolism by revealing that extrinsic FAs are taken up and accumulate in CRC. Inhibition of FA uptake and oxidation reduces proliferation of CRC cell lines and patient-derived organoids, providing strong evidence for an in vivo relevance of dietary FAs in tumour initiation and progression. It will be fascinating to explore to what extent and how gut microbes interact with FA metabolism in CRC to drive tumour development. Future research will show whether targeting CRC FA uptake and metabolism opens new therapeutic avenues.

Author affiliations
[1]Department of Surgery, TUM University Hospital Rechts der Isar, München, Germany
[2]Institute for Laboratory Animal Science, Hannover Medical School, Hannover, Germany
[3]Core Facility Microbiome, ZIEL – Institute for Food & Health, Technical University of Munich, Freising, Germany
[4]Functional Lipidomics and Metabolism Research, Institute of Clinical Chemistry and Laboratory Medicine, University Hospital Regensburg, Regensburg, Germany
[5]BioVariance GmbH, Waldsassen, Germany
[6]Institute of Clinical Chemistry and Laboratory Medicine, University Hospital Regensburg, Regensburg, Germany
[7]Functional Microbiome Research Group, Institute of Medical Microbiology, RWTH University Hospital, Aachen, Germany
[8]Chair of Nutrition and Immunology, Technical University of Munich, Munich, Germany

Acknowledgements We thank Doreen Mueller, Renate Kick, Dagmar Alzinger, Anna Smoczek, Johannes Plagge, Sven Hermeling and Leonie Roithmeier for excellent experimental support.

Contributors JE is the guarantor of the article. Conceptualisation: KPJ, JE. Methodology: KPJ, JS, GL, MB, RB, JE. Software: JS. Validation: KPJ, JS, GL, RB, JE. Formal analysis: KPJ, JE. Investigation: KPJ, AM, FJ, SG, AB, JS, GL, RB, SBo, SBr, TC, EW, OIC, KN, DH, SK, JE. Resources: KPJ, JE. Data curation: KPJ, JS, JE. Writing – Original Draft: KPJ, JE. Writing – Review and Editing: KPJ, AM, JS, GL, MB, RB, JE. Visualisation: KPJ, AM, JS, JE. Supervision: JE. Project administration: JE. Funding acquisition: KPJ, JE.

Funding We acknowledge the funding body of this work: Deutsche Forschungsgemeinschaft (DFG, German Research Foundation) Collaborative Research Center CRC 1371 (Microbiome signatures: functional relevance in the digestive tract; project no. 395357507; P13 to JE and KPJ).

Competing interests None declared.

Patient and public involvement Patients and/or the public were not involved in the design, or conduct, or reporting, or dissemination plans of this research.

Patient consent for publication Not applicable.

Ethics approval This study involves human participants. The use of human tissue samples was approved by the Ethics Committee of the School of Medicine and Health, TUM (#1926/07; #5428/12, #375-16S, #2022-169-S-KH), with informed consent by all participants. All mouse experiments were approved (Regierung von Oberbayern, approval numbers: 55.2-1-54-2532-192-2016, ROB-55.2-2532. Vet_02-21-124; Niedersächsisches Landesamt für Verbraucherschutz und Lebensmittelsicherheit, approval number: 18/2895; Landesamt für Natur, Umwelt und Verbraucherschutz Nordrhein-Westfalen; approval numbers: 81-02.04.2018. A396, 81-02.04.2018.A425).

Provenance and peer review Not commissioned; externally peer reviewed.

Data availability statement Data are available upon reasonable request. All data relevant to the study are included in the article or uploaded as supplementary information. Not applicable.

ORCID iDs
Klaus Peter Janssen https://orcid.org/0000-0002-4707-7887
Silvia Bolsega https://orcid.org/0009-0003-8290-8214
Amira Metwaly https://orcid.org/0000-0001-5740-0230
Sophia von Gamm https://orcid.org/0009-0006-3064-6162
Klaus Neuhaus https://orcid.org/0000-0002-6020-2814
Sarah Brunner https://orcid.org/0000-0002-3293-1657
Thomas Clavel https://orcid.org/0000-0002-7229-5595
Dirk Haller https://orcid.org/0000-0002-6977-4085
Josef Ecker https://orcid.org/0000-0003-4799-0788

REFERENCES

1 Soundararajan R, Maurin MM, Rodriguez-Silva J, *et al*. Integration of lipidomics with targeted, single cell, and spatial transcriptomics defines an unresolved pro-inflammatory state in colon cancer. *Gut* 2025;74:586–602.
2 Lee-Okada HC, Xue C, Yokomizo T. Recent advances on the physiological and pathophysiological roles of polyunsaturated fatty acids and their biosynthetic pathway. *Biochim Biophys Acta Mol Cell Biol Lipids* 2025;1870:159564.
3 Pavlova NN, Zhu J, Thompson CB. The hallmarks of cancer metabolism: Still emerging. *Cell Metab* 2022;34:355–77.
4 Baenke F, Peck B, Miess H, *et al*. Hooked on fat: the role of lipid synthesis in cancer metabolism and tumour development. *Dis Model Mech* 2013;6:1353–63.
5 Ecker J, Benedetti E, Kindt ASD, *et al*. The Colorectal Cancer Lipidome: Identification of a Robust Tumor-Specific Lipid Species Signature. *Gastroenterology* 2021;161:910–23.
6 Zaytseva YY, Rychahou PG, Le A-T, *et al*. Preclinical evaluation of novel fatty acid synthase inhibitors in primary colorectal cancer cells and a patient-derived xenograft model of colorectal cancer. *Oncotarget* 2018;9:24787–800.
7 Peck B, Schulze A. Lipid Metabolism at the Nexus of Diet and Tumor Microenvironment. *Trends Cancer* 2019;5:693–703.
8 Ecker J, Scherer M, Schmitz G, *et al*. A rapid GC-MS method for quantification of positional and geometric isomers of fatty acid methyl esters. *J Chromatogr B Analyt Technol Biomed Life Sci* 2012;897:98–104.
9 Kindt A, Liebisch G, Clavel T, *et al*. The gut microbiota promotes hepatic fatty acid desaturation and elongation in mice. *Nat Commun* 2018;9:3760.
10 Hellerstein MK, Neese RA. Mass isotopomer distribution analysis at eight years: theoretical, analytic, and experimental considerations. *Am J Physiol* 1999;276:E1146–70.
11 Ecker J, Liebisch G. Application of stable isotopes to investigate the metabolism of fatty acids, glycerophospholipid and sphingolipid species. *Prog Lipid Res* 2014;54:14–31.
12 Hohmann M, Brunner V, Johannes W, *et al*. Bacillamide D produced by Bacillus cereus from the mouse intestinal bacterial collection (miBC) is a potent cytotoxin in vitro. *Commun Biol* 2024;7:655.
13 Yin Y, Sichler A, Ecker J, *et al*. Gut microbiota promote liver regeneration through hepatic membrane phospholipid biosynthesis. *J Hepatol* 2023;78:820–35.
14 Reitmeier S, Kiessling S, Neuhaus K, *et al*. Comparing Circadian Rhythmicity in the Human Gut Microbiome. *STAR Protoc* 2020;1:100148.
15 Janssen K-P, Alberici P, Fsihi H, *et al*. APC and oncogenic KRAS are synergistic in enhancing Wnt signaling in intestinal tumor formation and progression. *Gastroenterology* 2006;131:1096–109.
16 Mukund K, Syulyukina N, Ramamoorthy S, *et al*. Right and left-sided colon cancers - specificity of molecular mechanisms in tumorigenesis and progression. *BMC Cancer* 2020;20:317.
17 Arai J, Hayakawa Y, Koike K. The Colorectal Cancer Lipidome: Are There Any Differences in Lipid Species Between Right and Left Colorectal Cancers? *Gastroenterology* 2022;162.
18 Lee MS, Menter DG, Kopetz S. Right Versus Left Colon Cancer Biology: Integrating the Consensus Molecular Subtypes. *J Natl Compr Canc Netw* 2017;15:411–9.
19 Höring M, Brunner S, Scheiber J, *et al*. Sex-specific response of the human plasma lipidome to short-term cold exposure. *Biochim Biophys Acta Mol Cell Biol Lipids* 2025;1870:159567.
20 Sales S, Graessler J, Ciucci S, *et al*. Gender, Contraceptives and Individual Metabolic Predisposition Shape a Healthy Plasma Lipidome. *Sci Rep* 2016;6:27710.
21 Mittendorfer B, Patterson BW, Klein S. Effect of sex and obesity on basal VLDL-triacylglycerol kinetics. *Am J Clin Nutr* 2003;77:573–9.
22 Majek O, Gondos A, Jansen L, *et al*. Sex differences in colorectal cancer survival: population-based analysis of 164,996 colorectal cancer patients in Germany. *PLoS One* 2013;8:e68077.
23 Siegel RL, Torre LA, Soerjomataram I, *et al*. Global patterns and trends in colorectal cancer incidence in young adults. *Gut* 2019;68:2179–85.
24 Åbacka H, Masoni S, Poli G, *et al*. SMS121, a new inhibitor of CD36, impairs fatty acid uptake and viability of acute myeloid leukemia. *Sci Rep* 2024;14:9104.
25 Glatz JFC, Nabben M, Luiken JJFP. CD36 (SR-B2) as master regulator of cellular fatty acid homeostasis. *Curr Opin Lipidol* 2022;33:103–11.
26 Ceccarelli SM, Chomienne O, Gubler M, *et al*. Carnitine palmitoyltransferase (CPT) modulators: a medicinal chemistry perspective on 35 years of research. *J Med Chem* 2011;54:3109–52.
27 Burkhardt R, Ecker J. A tripartite alliance for dietary fat absorption. *Science* 2025;390:128–9.
28 Gao Y, Kennelly JP, Xiao X, *et al*. T cell cholesterol transport links intestinal immune responses to dietary lipid absorption. *Science* 2025;390:eadt4169.
29 Araújo JR, Tazi A, Burlen-Defranoux O, *et al*. Fermentation Products of Commensal Bacteria Alter Enterocyte Lipid Metabolism. *Cell Host Microbe* 2020;27:358–75.
30 Martinez-Guryn K, Hubert N, Frazier K, *et al*. Small Intestine Microbiota Regulate Host Digestive and Absorptive Adaptive Responses to Dietary Lipids. *Cell Host Microbe* 2018;23.
31 Santiago P, Melo T, Barceló-Nicolau M, *et al*. Advancing colorectal cancer research through lipidomics. *Mol Omics* 2025;21:373–89.
32 Kitamura C, Sonoda H, Nozawa H, *et al*. The component changes of lysophospholipid mediators in colorectal cancer. *Tumour Biol* 2019;41:1010428319848616.
33 Mika A, Kobiela J, Czumaj A, *et al*. Hyper-Elongation in Colorectal Cancer Tissue - Cerotic Acid is a Potential Novel Serum Metabolic Marker of Colorectal Malignancies. *Cell Physiol Biochem* 2017;41:722–30.
34 Zheng R, Xiong L, Wang J, *et al*. Direct MS enabled discovery of lipid signatures with diagnostic implications in colorectal cancer. *J Pharm Biomed Anal* 2026;268:117198.
35 Zhang J, Zhang L, Ye X, *et al*. Characteristics of fatty acid distribution is associated with colorectal cancer prognosis. *Prostaglandins Leukot Essent Fatty Acids* 2013;88:355–60.
36 Guo S, Wang Y, Zhou D, *et al*. Significantly increased monounsaturated lipids relative to polyunsaturated lipids in six types of cancer microenvironment are observed by mass spectrometry imaging. *Sci Rep* 2014;4:5959.
37 Lian J, Duan X, Chen W, *et al*. Targeting FADS1-mediated lipid metabolism and signaling: a novel therapeutic strategy for precision oncology in colorectal and esophageal cancers. *Cell Death Discov* 2025;11:460.
38 Serra-Majem L, Nissensohn M, Øverby NC, *et al*. Dietary methods and biomarkers of omega 3 fatty acids: a systematic review. *Br J Nutr* 2012;107:S64–76.

39 Vonk RJ, Kalivianakis M, Minich DM, *et al*. The metabolic importance of unabsorbed dietary lipids in the colon. *Scand J Gastroenterol Suppl* 1997;222:65–7.
40 Arai J, Suzuki N, Niikura R, *et al*. Chemoprevention for Colorectal Cancers: Are Chemopreventive Effects Different Between Left and Right Sided Colorectal Cancers? *Dig Dis Sci* 2022;67:5227–38.
41 Dove WF, Clipson L, Gould KA, *et al*. Intestinal neoplasia in the ApcMin mouse: independence from the microbial and natural killer (beige locus) status. *Cancer Res* 1997;57:812–4.
42 Li Y, Kundu P, Seow SW, *et al*. Gut microbiota accelerate tumor growth via c-jun and STAT3 phosphorylation in APCMin/+ mice. *Carcinogenesis* 2012;33:1231–8.
43 Belcheva A, Irrazabal T, Robertson SJ, *et al*. Gut microbial metabolism drives transformation of MSH2-deficient colon epithelial cells. *Cell* 2014;158:288–99.
44 Coleman OI, Sorbie A, Riva A, *et al*. ATF6 activation alters colonic lipid metabolism causing tumour-associated microbial adaptation. *Nat Metab* 2025;7:1830–50.
45 Kostic AD, Chun E, Meyerson M, *et al*. Microbes and inflammation in colorectal cancer. *Cancer Immunol Res* 2013;1:150–7.
46 Holtorf A, Conrad A, Holzmann B, *et al*. Cell-type specific MyD88 signaling is required for intestinal tumor initiation and progression to malignancy. *Oncoimmunology* 2018;7:e1466770.
47 Baas FS, Brusselaers N, Nagtegaal ID, *et al*. Navigating beyond associations: Opportunities to establish causal relationships between the gut microbiome and colorectal carcinogenesis. *Cell Host Microbe* 2024;32:1235–47.
48 Gao Z, Guo B, Gao R, *et al*. Microbiota disbiosis is associated with colorectal cancer. *Front Microbiol* 2015;6:20.
49 Stecher B. The Roles of Inflammation, Nutrient Availability and the Commensal Microbiota in Enteric Pathogen Infection. *Microbiol Spectr* 2015;3.
50 Flemer B, Lynch DB, Brown JMR, *et al*. Tumour-associated and non-tumour-associated microbiota in colorectal cancer. *Gut* 2017;66:633–43.
51 Costa CP da, Vieira P, Mendes-Rocha M, *et al*. The Tissue-Associated Microbiota in Colorectal Cancer: A Systematic Review. *Cancers (Basel)* 2022;14:3385.
52 Tosolini M, Kirilovsky A, Mlecnik B, *et al*. Clinical impact of different classes of infiltrating T cytotoxic and helper cells (Th1, th2, treg, th17) in patients with colorectal cancer. *Cancer Res* 2011;71:1263–71.
53 Brown EM, Clardy J, Xavier RJ. Gut microbiome lipid metabolism and its impact on host physiology. *Cell Host Microbe* 2023;31:173–86.
54 Haque S, Bantun F, Jalal NA, *et al*. Gut microbiota alterations and their association with tumorigenic pathways in colorectal cancer: insights from a pooled analysis of 109 microbiome datasets. *Gut Pathog* 2025;17:82.
55 Lo C-H, Wu D-C, Jao S-W, *et al*. Enrichment of Prevotella intermedia in human colorectal cancer and its additive effects with Fusobacterium nucleatum on the malignant transformation of colorectal adenomas. *J Biomed Sci* 2022;29:88.
56 Wang X, Chen H, Yang M, *et al*. Influence of gut microbiota and immune markers in different stages of colorectal adenomas. *Front Microbiol* 2025;16:1556056.
57 Xiang Y, Zhang C, Wang J, *et al*. Identification of host gene-microbiome associations in colorectal cancer patients using mendelian randomization. *J Transl Med* 2023;21:535.